Adsorption (2020) 26:375–386
https://doi.org/10.1007/s10450-019-00185-4

An activity-based formulation for Langmuir adsorption isotherm

Chun-Kai Chang[1] · Hla Tun[2] · Chau-Chyun Chen[2]

Received: 11 June 2019 / Revised: 23 October 2019 / Accepted: 20 November 2019 / Published online: 27 November 2019

Abstract
This work presents an activity-based formulation for Langmuir adsorption isotherm. Treating adsorption as a chemical reaction between the gas molecule and the adsorption vacant site, the classical Langmuir isotherm model expresses the reaction in terms of the species concentrations. Designed to capture the surface heterogeneity, the proposed thermodynamic Langmuir isotherm model substitutes the species concentrations with the species activities and calculates the species activity coefficients with the adsorption non-random two-liquid activity coefficient model. The resulting isotherm model accurately represents pure component adsorption isotherms for gases with wide varieties of adsorbents including silica gels, activated carbons, zeolites and metal organic frameworks at various temperatures. With three physically meaningful parameters, the model outperforms the classical Langmuir isotherm model for the 98 isotherms of 33 systems examined.

Keywords Activity coefficient · Adsorption · Adsorption non-random two-liquid theory · Langmuir isotherm · Thermodynamic Langmuir isotherm

1 Introduction

Adsorption is widely practiced in industrial processes for molecule separations by taking advantages of the difference in adsorbate molecule affinity to adsorbents (Li et al. 2009). To support process research and development, many researchers have pursued development of empirical or semi-empirical engineering correlations or models for both pure component and mixed-gas adsorption equilibria (Myers and Prausnitz 1965; Mathias et al. 1996; Myers 2005; Talu and Zwiebel 1986; Walton and Sholl 2015). Successful engineering models for adsorption equilibria are expected to (1) be thermodynamically consistent, (2) require few adjustable model parameters, (3) be applicable to both pure component adsorption isotherms and mixed-gas adsorption isotherms, and (4) calculate mixed-gas adsorption isotherms from pure component adsorption isotherms (Sircar 1991). While adsorption equilibria of a single gas on an adsorbent represents the simplest case of adsorption processes, accurate correlation of pure component adsorption isotherms remains a challenge due to adsorbent surface heterogeneity (Sircar 1991).

The classical Langmuir isotherm model (Langmuir 1918) is considered the first scientifically sound expression for pure component adsorption isotherms:

$$n_i = n_i^0 \frac{KP}{1 + KP} \tag{1}$$

where n_i is the adsorption amount of gas component i; n_i^0 is the adsorption maximum amount; P is the gas vapor pressure. Indicative of the affinity between adsorbate and adsorbent, K is the apparent adsorption equilibrium constant. The Langmuir isotherm has been successfully used to describe adsorption behavior of many systems such as adsorption of non-polar gases on activated carbons and zeolites. Ignoring the surface heterogeneity and the van der Waals interactions between adsorbates and adsorbents (Sreńscek-Nazzal et al. 2015; Foo and Hameed 2010), the Langmuir isotherm may be inadequate in describing pure component adsorption isotherms especially at low temperature and high pressure regions (Benard and Chahine 1997). (see Supporting Information. Figs. S1 and S2 for examples).

Electronic supplementary material The online version of this article (https://doi.org/10.1007/s10450-019-00185-4) contains supplementary material, which is available to authorized users.

✉ Chau-Chyun Chen
chauchyun.chen@ttu.edu

[1] Department of Chemical Engineering, National Taiwan University, Taipei 10617, Taiwan

[2] Department of Chemical Engineering, Texas Tech University, Lubbock, TX 79409-3121, USA

Among the many efforts (Sips 1948, 1950; Toth 1971) to improve upon the classical Langmuir isotherm model, the empirical Sips isotherm model (Sips 1948, 1950) probably is the most successful one. Following Freundlich isotherm (Freundlich 1907), Sips introduced an empirical "heterogeneity" parameter m, which is usually less than unity (Pakseresht et al. 2002), to the Langmuir isotherm. Shown in Eq. 2, the resulting Sips isotherm expression is much more flexible in representing adsorption isotherm data.

$$n_i = n_i^0 \frac{(KP)^m}{1 + (KP)^m} \tag{2}$$

With three adjustable parameters (n_i^0, K and m), the Sips isotherm expression and other similar empirical expressions are capable of correlating pure component adsorption isotherm data much better than the Langmuir isotherm could achieve with two adjustable parameters (n_i^0 and K). However, the introduction of empirical heterogeneity parameter m distorts the theoretical basis of the classical Langmuir isotherm and the physical significance of the Langmuir isotherm parameters (n_i^0 and K) is lost.

Instead of pursuing empirical corrections of the classical Langmuir isotherm to address the issue of surface heterogeneity, this work re-examines the theoretical basis of the Langmuir isotherm and proposes an activity-based formulation for the isotherm. The reformulation is achieved by substituting the concentrations of both the vacant sites and the occupied sites with the site activities. Specifically, the surface heterogeneity is treated as a departure from ideal adsorbate phase solution. The reference state for the vacant sites is at zero surface coverage while the reference state for the occupied sites is at full surface coverage. The site activities are further calculated with the adsorption non-random two-liquid (aNRTL) activity coefficient model (Kaur et al. 2019). Derived from the two fluid theory (Renon and Prausnitz 1968; Ravichandran et al. 2018) and the assumption that the adsorbate phase nonideality is dominated by adsorbate-adsorbent interactions, the aNRTL model has been shown to successfully correlate and predict wide varieties of mixed-gas adsorption isotherms with a single binary interaction parameter per adsorbate–adsorbate pair. The resulting activity-based Langmuir isotherm, called "thermodynamic Langmuir isotherm" in this work, should represent a theoretically rigorous refinement of the classical Langmuir isotherm. The model parameters include n_i^0, the adsorption maximum, $K°$, the thermodynamic adsorption equilibrium constant, and τ, the aNRTL binary interaction parameter.

The subsequent sections present the formulation of the thermodynamic Langmuir isotherm, the adsorption NRTL activity coefficient model, and the model results for 98 pure component adsorption isotherms for adsorbents including silica gels, activated carbons, zeolites and metal organic frameworks (MOFs). Also presented are the results with the classical Langmuir isotherm and the Sips isotherm. Lastly, the physical interpretation of the thermodynamic Langmuir isotherm model parameters is discussed.

2 Theory

2.1 Thermodynamic Langmuir isotherm

The classical Langmuir adsorption isotherm equation is derived from reaction kinetics (Sohn and Kim 2005). Suppose there is an adsorption and desorption reaction of pure gas A:

$$A_{(g)} + S \leftrightarrow AS \tag{3}$$

where S stands for the vacant sites and AS the occupied sites with gas A. When this reaction reaches chemical equilibrium state at pressure P, the rates of adsorption and desorption are the same.

$$k_a P[S] = k_d[AS] \tag{4}$$

where k_a is the rate constant of adsorption, k_d is the rate constant of desorption, $[S]$ is the vacant site concentration, and $[AS]$ is the occupied site concentration. The apparent chemical equilibrium constant, K, can be written as:

$$K = \frac{k_a}{k_d} = \frac{[AS]}{P[S]} = \frac{n_1}{\left(n_1^0 - n_1\right)P} = \frac{x_1}{\left(1 - x_1\right)P} \tag{5}$$

where n_1 stands for the adsorption amount of adsorbed gas component 1, n_1^0 stands for the adsorption maximum, and x_1 stands for the adsorption extent, i.e., the ratio of n_1 and n_1^0. Langmuir isotherm equation, Eq. 1, can be obtained after solving for x_1. Note that here we denote gas A and gas component 1 interchangeably.

The Langmuir isotherm assumes the adsorption and desorption rates are proportional to the concentrations of vacant sites and occupied sites respectively. In other words, the model ignores the "heterogeneity" of the adsorption sites and the apparent chemical equilibrium constant, K, should be a function of the surface coverage, or the adsorption extent, x_1. To account for the "heterogeneity" of the adsorption sites and to achieve a rigorous thermodynamic formulation of Langmuir isotherm, this work substitutes the site concentrations in Eq. 5 with the site activities, i.e., the product of site concentration and site activity coefficient. See Eq. 6.

$$K° = \frac{k_a}{k_d} = \frac{a_{AS}}{Pa_S} = \frac{\gamma_1 x_1}{\gamma_\phi \left(1 - x_1\right)P} \tag{6}$$

here $K°$ is the thermodynamic adsorption equilibrium constant, a_{AS} is the activity of the occupied sites with adsorbed

gas A, a_S is the activity of the vacant sites, and γ_1 and γ_ϕ are the activity coefficient of the occupied sites with adsorbed gas component 1 and the activity coefficient of the vacant sites, respectively. The reference state for the occupied sites with adsorbed gas component 1 is chosen to be at full surface coverage, i.e., saturated adsorption state with $x_1 = 1$. The reference state for the vacant sites is chosen to be at zero surface coverage, i.e., the vacant adsorption state with $x_1 = 0$. In other words, $\gamma_1 = 1$ at $x_1 = 1$, and $\gamma_\phi = 1$ at $x_1 = 0$.

Reformulating Eq. 6, one obtains the following implicit adsorption isotherm expression.

$$n_1 = n_1^0 \frac{K^\circ \gamma_\phi P}{\gamma_1 + K^\circ \gamma_\phi P} \tag{7}$$

here γ_1 and γ_ϕ are functions of x_1. The relationship between the thermodynamic adsorption equilibrium constant K° and the apparent adsorption equilibrium constant K is shown in Eq. 8.

$$K(x_1) = K^\circ \frac{\gamma_\phi(x_1)}{\gamma_1(x_1)} \tag{8}$$

Equation 7 is referred to as the "thermodynamic Langmuir isotherm model". The classical Langmuir isotherm is recovered if both the activity coefficients of the occupied sites and the vacant sites are unity. However, the surface heterogeneity suggests there are vacant sites with stronger adsorption potential and vacant sites with weaker adsorption potential. It is expected that the vacant sites with stronger adsorption potential should be occupied before the sites with weaker adsorption potential. Therefore, the activity coefficient of vacant sites should start with unity at zero surface coverage (reference state) and decline and deviate from unity as the adsorption extent increases. To the contrary, the activity coefficient of occupied sites should increase and approach unity as the adsorption proceeds to full surface coverage (reference state). In other words, we expect negative deviations from ideal solution behavior for both the vacant sites and the occupied sites.

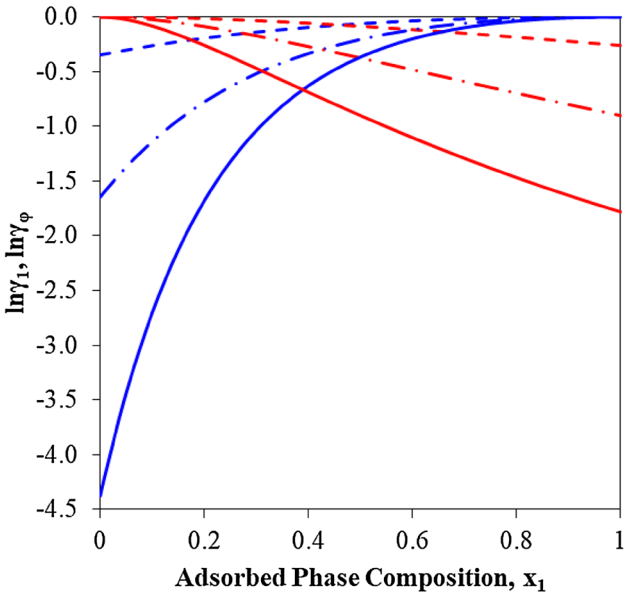

Fig. 1 Site activity coefficients as functions of adsorption extent with different $\tau_{1\phi}$ ($\alpha = 0.3$): $\tau_{1\phi}$ =-1 (dashed line), $\tau_{1\phi}$ =-2 (dotted dashed line) and $\tau_{1\phi}$ =-3 (solid line); blue lines stand for activity coefficients of occupied sites with adsorbate gas '1' and red lines stand for activity coefficients of vacant sites with phantom molecule 'φ'

2.2 The adsorption NRTL activity coefficient model

The aNRTL model activity coefficient expressions (Kaur et al. 2019) for two competing adsorbate components 1 and 2 on the adsorbate phase are as follows.

$$\ln \gamma_1 = x_2^2 \left[\tau_{12} \frac{(G_{12} - 1)}{(x_2 + x_1 G_{12})^2} \right] \tag{9a}$$

$$\ln \gamma_2 = x_1^2 \left[\tau_{21} \frac{(G_{21} - 1)}{(x_1 + x_2 G_{21})^2} \right] \tag{9b}$$

with

$$G_{12} = \exp(-\alpha \tau_{12}) \tag{10a}$$

$$G_{21} = \exp(-\alpha \tau_{21}) \tag{10b}$$

and

$$\tau_{12} = -\tau_{21} = \frac{g_{10} - g_{20}}{RT} \tag{11}$$

where g_{10} is the interaction potential between adsorbate 1 and adsorbent 0, g_{20} is the interaction potential between adsorbate 2 and adsorbent 0, R is gas constant, T is temperature, and α is the non-randomness parameter. Following the convention of NRTL model (Renon and Prausnitz 1968), α is fixed at 0.3 in this study. τ_{12} is the binary interaction parameter for the pair of adsorbates 1 and 2.

To apply the adsorption NRTL model, we follow the concept of "competition" between two adsorbate components 1 and 2 in mixed-gas adsorption equilibria. Specifically, we consider pure component adsorption equilibria as a "competition" between adsorbate component 1 and a phantom molecule ϕ. In other words, while the occupied sites are covered with adsorbate component 1, the vacant sites are "covered" with phantom molecule ϕ. Therefore, the adsorption NRTL model becomes

Table 1 Comparison of root mean square errors among Langmuir, Sips and thermodynamic Langumir

System no.	Gas	Adsorbent	T (K)	Langmuir *RMS* (mmol/g)	Sips *RMS* (mmol/g)	Thermodynamic Langmuir *RMS* (mmol/g)	Experimental data source
1	CH_4	Activated carbon	212.7	0.283	0.048	0.052	Reich et al. (1980)
			260.2	0.128	0.028	0.027	
			301.4	0.047	0.022	0.024	
2	CH_4	Zeolite 5A	273	0.011	0.009	0.008	Bakhtyari and Mofarahi (2014)
			303	0.012	0.011	0.012	
			343	0.005	0.005	0.005	
3	CH_4	Zeolite 13X	298	0.109	0.054	0.040	Cavenati et al. (2004)
			308	0.093	0.049	0.034	
			323	0.036	0.029	0.029	
4	CH_4	UiO-66	273	0.003	0.002	0.003	Zhang et al. (2012)
			298	0.001	0.001	0.001	
			323	0.004	0.003	0.003	
5	CH_4	Zn-MOF	273	0.114	0.019	0.096	Mu and Walton (2011)
			282	0.102	0.016	0.094	
			298	0.084	0.018	0.084	
6	C_2H_4	Silica gel	273.15	0.031	0.009	0.009	Lewis et al. (1950)
			298.15	0.009	0.007	0.007	
			313.15	0.009	0.003	0.006	
7	C_2H_4	Zeolite 5A	283	0.119	0.034	0.100	Mofarahi and Salehi (2013)
			303	0.054	0.023	0.021	
			323	0.053	0.014	0.017	
8	C_2H_6	Silica gel	278	0.062	0.029	0.037	Olivier and Jadot (1997)
			293	0.051	0.038	0.036	
			303	0.034	0.020	0.034	
9	C_2H_6	Zeolite 5A	283	0.060	0.057	0.060	Mofarahi and Salehi (2013)
			303	0.029	0.029	0.029	
			323	0.023	0.018	0.018	
10	C_3H_6	Silica gel	273.15	0.077	0.038	0.037	Lewis et al. (1950)
			298.15	0.066	0.056	0.056	
			313.15	0.051	0.011	0.003	
11	C_3H_6	Activated carbon	303.15	0.412	0.060	0.061	Laukhuf and Plank (1969)
			313.15	0.354	0.127	0.128	
			323.15	0.314	0.047	0.051	
12	C_3H_6	Zeolite 13X	323	0.086	0.010	0.062	Campo et al. (2013)
			373	0.177	0.042	0.066	
			423	0.101	0.019	0.018	
13	C_3H_6	Cu-BTC	323	0.349	0.223	0.349	Ferreira et al. (2011)
			348	0.131	0.085	0.131	
			373	0.124	0.044	0.124	
14	C_3H_8	Silica gel	273.15	0.064	0.013	0.030	Lewis et al. (1950)
			298.15	0.030	0.011	0.019	
			313.15	0.017	0.010	0.012	
15	C_3H_8	Activated carbon	293.15	0.413	0.129	0.399	Payne et al. (1968)
			303.15	0.497	0.069	0.110	
			313.15	0.401	0.060	0.097	

Table 1 (continued)

System no.	Gas	Adsorbent	T (K)	Langmuir *RMS* (mmol/g)	Sips *RMS* (mmol/g)	Thermodynamic Langmuir *RMS* (mmol/g)	Experimental data source
16	C_3H_8	Zeolite 13X	323	0.034	0.017	0.020	Campo et al. (2013)
			373	0.070	0.047	0.050	
			423	0.033	0.025	0.033	
17	C_3H_8	Cu-BTC	323	0.216	0.119	0.216	Ferreira et al. (2011)
			348	0.123	0.064	0.123	
			373	0.086	0.032	0.086	
18	i-C4H10	Zeolite 13X	298.15	0.106	0.050	0.066	Hyun and Danner (1982)
			323.15	0.053	0.028	0.020	
			373.15	0.031	0.031	0.031	
19	i-C4H10	Cu-BTC	323	0.239	0.071	0.239	Ferreira et al. (2011)
			348	0.182	0.067	0.182	
			373	0.175	0.045	0.175	
20	C_5H_{12}	Activated carbon	333	0.222	0.039	0.071	Do and Do (2002)
			353	0.206	0.022	0.046	
			423	0.135	0.011	0.012	
21	C_5H_{12}	Zeolite 5A	373	0.033	0.006	0.006	Silva and Rodrigues (1997)
			423	0.034	0.006	0.009	
			473	0.059	0.006	0.006	
22	CO_2	Silica gel	283.15	0.008	0.003	0.005	Wang and LeVan (2009)
			298.15	0.005	0.002	0.004	
			313.15	0.003	0.001	0.002	
23	CO_2	Activated carbon	273.15	0.069	0.010	0.054	Zhang et al. (2013)
			298.15	0.029	0.007	0.024	
			348.15	0.008	0.004	0.007	
24	CO_2	Zeolite 5A	228.15	0.425	0.056	0.040	Wang and LeVan (2009)
			273.15	0.339	0.030	0.023	
			323.15	0.183	0.019	0.034	
			348.15	0.131	0.015	0.033	
25	CO_2	Zeolite 13X	298	0.555	0.076	0.139	Cavenati et al. (2004)
			308	0.523	0.110	0.075	
			323	0.388	0.103	0.231	
26	CO_2	Cu-BTC	293.15	0.100	0.060	0.100	Al-Janabi et al. (2015)
			333.15	0.067	0.018	0.067	
27	CO_2	UiO-66	273	0.019	0.012	0.018	Zhang et al. (2012)
			298	0.012	0.010	0.012	
			323	0.008	0.008	0.008	
28	CO_2	Zn-MOF	273	0.188	0.176	0.186	Mu and Walton (2011)
			282	0.175	0.162	0.174	
			298	0.103	0.085	0.095	
29	N_2	Activated carbon	298.15	0.002	0.002	0.002	Maring and Webley (2013)
			323.15	0.001	0.001	0.001	
			348.15	0.001	0.001	0.001	
30	N_2	Zeolite 5A	273	0.017	0.005	0.008	Bakhtyari and Mofarahi (2014)
			303	0.007	0.007	0.007	
			343	0.004	0.004	0.004	

Table 1 (continued)

System no.	Gas	Adsorbent	T (K)	Langmuir *RMS* (mmol/g)	Sips *RMS* (mmol/g)	Thermodynamic Langmuir *RMS* (mmol/g)	Experimental data source
31	N_2	Zeolite 13X	298	0.049	0.019	0.011	Cavenati et al. (2004)
			308	0.034	0.015	0.008	
			323	0.027	0.013	0.009	
32	N_2	Cu-BTC	293.15	0.006	0.006	0.006	Al-Janabi et al. (2015)
			333.15	0.008	0.008	0.008	
33	N_2	UiO-66	273	0.002	0.002	0.002	Zhang et al. (2012)
			298	0.001	0.001	0.001	
			323	0.001	0.001	0.001	

$$\ln \gamma_1 = x_\phi^2 \left[\tau_{1\phi} \frac{\left(G_{1\phi} - 1\right)}{\left(x_\phi + x_1 G_{1\phi}\right)^2} \right] \tag{12a}$$

$$\ln \gamma_\phi = x_1^2 \left[\tau_{\phi 1} \frac{\left(G_{\phi 1} - 1\right)}{\left(x_1 + x_\phi G_{\phi 1}\right)^2} \right] \tag{12b}$$

with

$$G_{1\phi} = \exp\left(-\alpha \tau_{1\phi}\right) \tag{13a}$$

$$G_{\phi 1} = \exp\left(-\alpha \tau_{\phi 1}\right) \tag{13b}$$

and

$$\tau_{1\phi} = -\tau_{\phi 1} = \frac{g_{10} - g_{\phi 0}}{RT} \tag{14}$$

where $x_\phi = 1 - x_1$, and g_{10} and $g_{\phi 0}$ are the interaction potential between component 1 and adsorbent 0 and the "interaction potential" between phantom molecule ϕ and adsorbent 0, respectively. Conceptually, $g_{\phi 0}$ may be considered as the potential field for the vacant sites.

As to be shown later, the binary interaction parameter $\tau_{1\phi}$ are found to be in the range of 0 to −5 for our test systems. The activity coefficients show negative deviation from ideality and the negative deviation increases as $\tau_{1\phi}$ becomes more negative, suggesting stronger attractive interaction between the adsorbate and the adsorbent (i.e., more negative g_{10}). Figure 1 illustrates the variations in activity coefficients with the adsorption extent as functions of $\tau_{1\phi}$. γ_1 shows negative deviation from unity in the beginning of adsorption process (weaker desorption potential) and approaches unity when the adsorption reaches saturation (reference state for the occupied sites). γ_ϕ shows an opposite trend from that of the occupied sites. γ_ϕ is unity in the beginning of adsorption process (reference state for the vacant cites) and then exhibits negative deviation from unity as the adsorption extent approaches saturation (weaker adsorption potential).

3 Results and discussion

We examine the model performance in correlating data for 98 selected pure component adsorption isotherms with the classical Langmuir isotherm model, the semi-empirical Sips isotherm model, and the thermodynamic Langmuir isotherm model. There are two adjustable parameters (n_i^0 and K) with the Langmuir isotherm, three adjustable parameters (n_i^0, K and m) with the Sips isotherm, and three adjustable parameters ($n_i^0, K°$ and $\tau_{1\phi}$) with the thermodynamic Langmuir isotherm.

The Maximum Likelihood Objective Function (Britt and Luecke 1973) is adopted in the regression of adsorption isotherm data. Specifically, the sum of square of the ratio of the difference between calculated n_i and experimental n_i to the expected standard deviation σ^{expt} (set to 0.05 mmol/g in this study) is minimized by adjusting the corresponding isotherm parameters.

$$Obj = \sum_i \left(\frac{n_i^{calc} - n_i^{expt}}{\sigma^{expt}} \right)^2 \tag{15}$$

where *Obj* is the objective function; superscripts *calc* and *expt* stand for calculated value and experimental data, respectively.

We use root mean square error (*RMS*) to evaluate the performance of the three isotherm models. The *RMS* is defined as following:

$$RMS = \sqrt{\frac{\sum_i \left(n_i^{calc} - n_i^{expt}\right)^2}{N}} \tag{16}$$

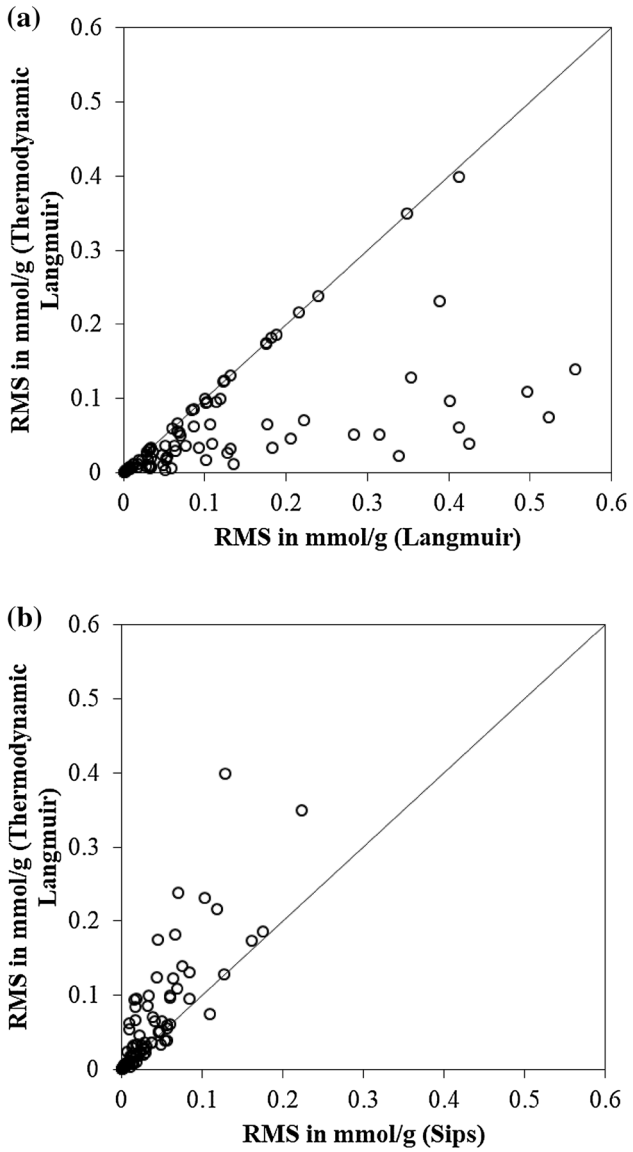

Fig. 2 Comparison of RMS with different models: **a** thermodynamic Langmuir compared to Langmuir, **b** thermodynamic Langmuir compared to Sips

where N is the number of data points for the adsorption isotherm.

Table 1 shows the corresponding *RMS* values with the models. Figure 2a and b show the *RMS* values for the isotherms with the new model plotted against those with the Langmuir isotherm and those with the Sips isotherm respectively. The results with the new model are superior to those with the Langmuir isotherm as all of the *RMS* data points are located in the lower right half corner of Fig. 2a. The new model is comparable to the Sips isotherm as Fig. 2b shows the *RMS* data points are mostly centered around the 45° line.

Figures 3a to c present the model results for CO_2, CH_4 and N_2 in zeolite 5A, respectively. Figure 3a shows the Langmuir isotherm fails to accurately describe the CO_2-zeolite 5A isotherm at 348.15 K (Wang and LeVan 2009) while the Sips isotherm and the new model fit the experimental data very well. All three models are able to fit the experimental data accurately for CH_4 and N_2 adsorption isotherms with zeolite 5A (Bakhtyari and Mofarahi 2014), as shown in Figs. 3b and c respectively. Figure 3d further shows the Langmuir isotherm fails to describe the CH_4 adsorption isotherm with activated carbon (Reich et al. 1980) while the isotherm is well represented with both the Sips isotherm and the thermodynamic Langmuir isotherm.

Tables S1 to S3 of Supporting Information report the regressed model parameters for Langmuir, Sips and the new model respectively. From the regressed parameters for Langmuir and for Sips, it becomes obvious that the Langmuir n_i^0 and K parameters can be distorted significantly when the "heterogeneity" parameter m is introduced in the Sips isotherm. The distortion is particularly pronounced when m is far from unity. Take CO_2 adsorption with activated carbon (Zhang et al. 2013) as an example, with $m \approx 0.85$, the Sips n_i^0 values are 4 to 6 times of the Langmuir n_i^0 values while the Sips K values are one order of magnitude less than that of the Langmuir K values.

By contrast, the thermodynamic Langmuir n_i^0 and $K°$ remain in line with the Langmuir n_i^0 and K. In fact, the thermodynamic Langmuir $K°$ is an intrinsic quantity and it is related to the Langmuir K with Eq. 8. Figure 4a and b show comparisons of the thermodynamic Langmuir $\ln K°$ and the Langmuir $\ln K$ for N_2 adsorption with zeolite 5A (Bakhtyari and Mofarahi 2014) and CH_4 adsorption with activated carbon (Reich et al. 1980) respectively. While the thermodynamic Langmuir $\ln K°$ remains constant at a given temperature, the Langmuir $\ln K$ decreases with the adsorption extent. It is worth noting that the $\tau_{1\phi}$ is near zero for the N_2/zeolite 5A system, the Langmuir $\ln K$ deviates only slightly from the thermodynamic Langmuir $\ln K°$, and the classical Langmuir should be able to capture the isotherm data well. To the contrary, the absolute value of $\tau_{1\phi}$ is significantly larger for the CH_4/activated carbon system, the Langmuir $\ln K$ deviates significantly from the thermodynamic Langmuir $\ln K°$, and the classical Langmuir would fail to describe the adsorption isotherm.

Given the thermodynamic Langmuir n_i^0 and $K°$, one may define a thermodynamic driving force for adsorption, or adsorption strength η, as the product of n_i^0 and $K°$.

$$\eta = n_i^0 K° \tag{16}$$

Figure 5a to c show the adsorption strength for CH_4, CO_2 and N_2 in various adsorbents respectively. The

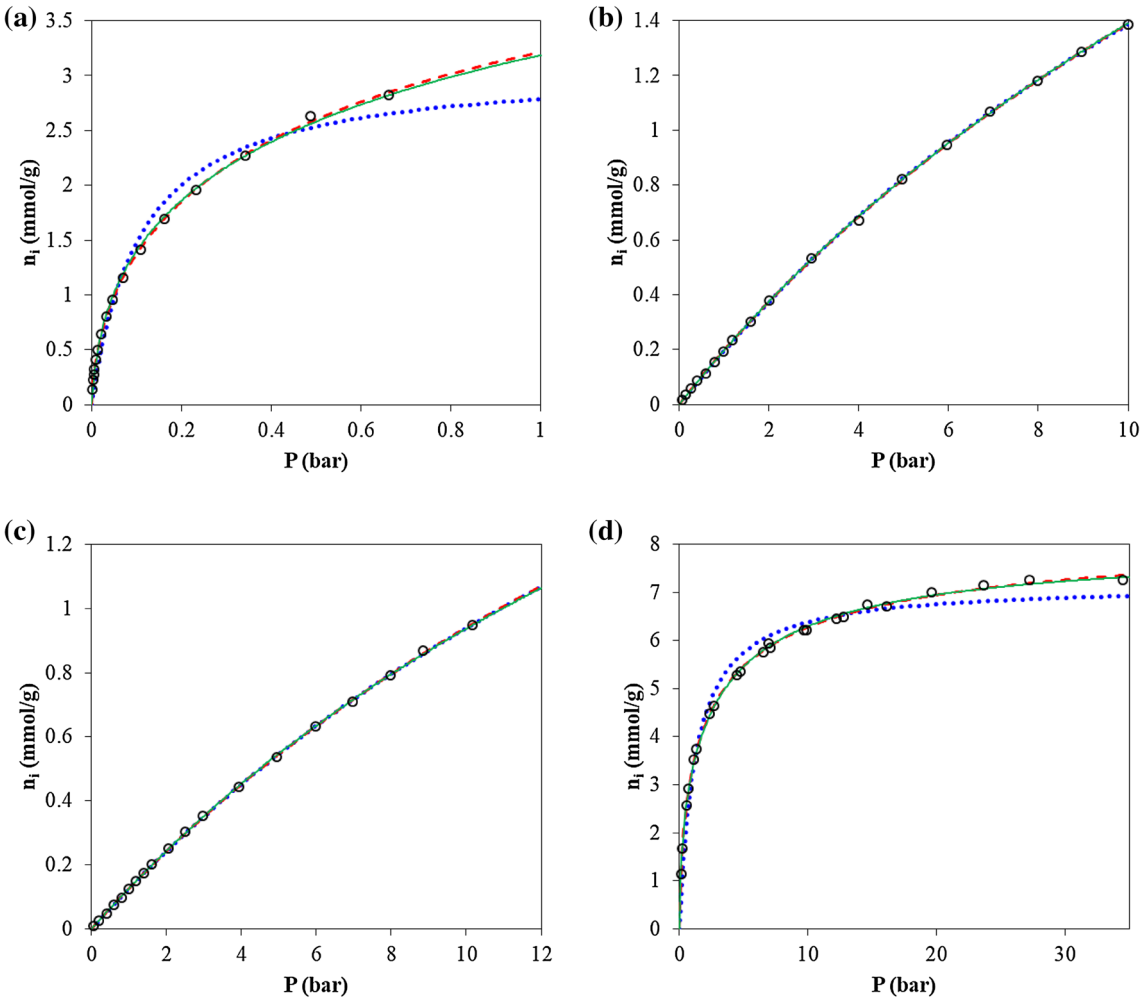

Fig. 3 Comparison of adsorption isotherms with different models: **a** CO_2/zeolite 5A (Wang and LeVan 2009) at 348.15 K, **b** CH_4/zeolite 5A (Bakhtyari and Mofarahi 2014) at 343 K, **c** N_2/zeolite 5A (Bakhtyari and Mofarahi 2014) at 343 K and **d** CH_4/activated carbon (Reich et al. 1980) at 212.7 K; experimental data (open circle), Langmuir (dotted blue line), Sips (dashed red line), and thermodynamic Langmuir (green solid line)

adsorption strength declines as temperature increases. η could be an effective measure to select adsorbents for a given separation task since the unit of η is adsorption amount per adsorbent unit mass per unit pressure. In other words, η has the same unit as the Henry's constant H. The relation between the Henry's constant H and the adsorption strength η can be obtained from Eq. 7 when the pressure is approaching zero:

$$H = \frac{\eta}{\gamma_1(P \to 0)} = \frac{\eta}{\gamma_1^{\infty}} \tag{17}$$

where γ_1^{∞} is the infinite dilution activity coefficient and always less than or equal to unity. Different from the Henry's constant, the adsorption strength is a measure of the intrinsic adsorption potential of the isotherm while the Henry's constant is a measure valid only at low pressures. Given η, for example, zeolite 5A is the strongest of the adsorbents shown in Fig. 5b for CO_2 adsorption.

While the new model is successful in capturing adsorption behavior of most systems, Table 1 shows that the thermodynamic Langmuir isotherm is not able to capture well the experimental data for systems with Cu-BTC MOF (Ferreira et al. 2011; Al-Janabi et al. 2015). The identified $\tau_{1\phi}$'s for these systems are all around zero, suggesting ideal solution behavior. The Sips isotherm is able to correlate the data slightly better, albeit with the Sips parameter m greater than unity. Figures 6a and b present the isotherms for C_3H_8 and i-C_4H_{10} adsorption with Cu-BTC (Ferreira et al. 2011) respectively. These isotherms show near step change behavior in reaching saturation. For these systems, the thermodynamic Langmuir isotherm initially overpredicts and then underpredicts n_i at the low adsorption region, and it predicts relatively well at the high adsorption region. To the contrary,

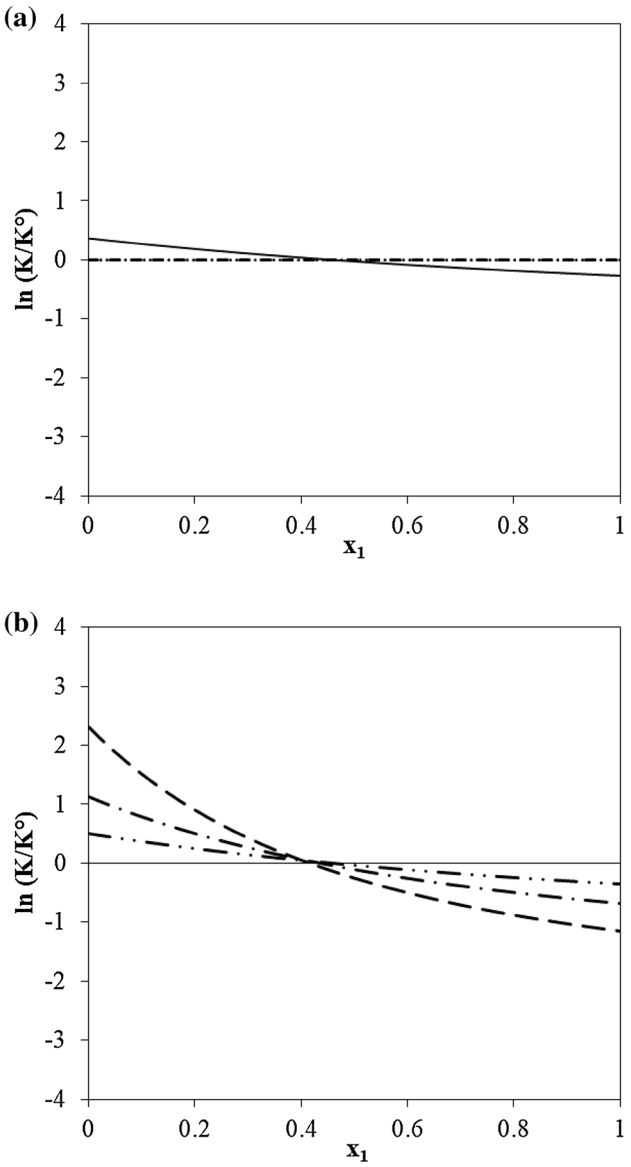

Fig. 4 ln $(K/K°)$ of **a** N_2/zeolite 5A (Bakhtyari and Mofarahi 2014) at 273 K (solid line), 303 K (thin dashed line), and 343 K (dotted line); **b** CH_4/activated carbon (Reich et al. 1980) at 212.7 K (thick dashed line), 260.2 K (thick dashed line with dot), and 301.4 K (thick dashed line with double dots)

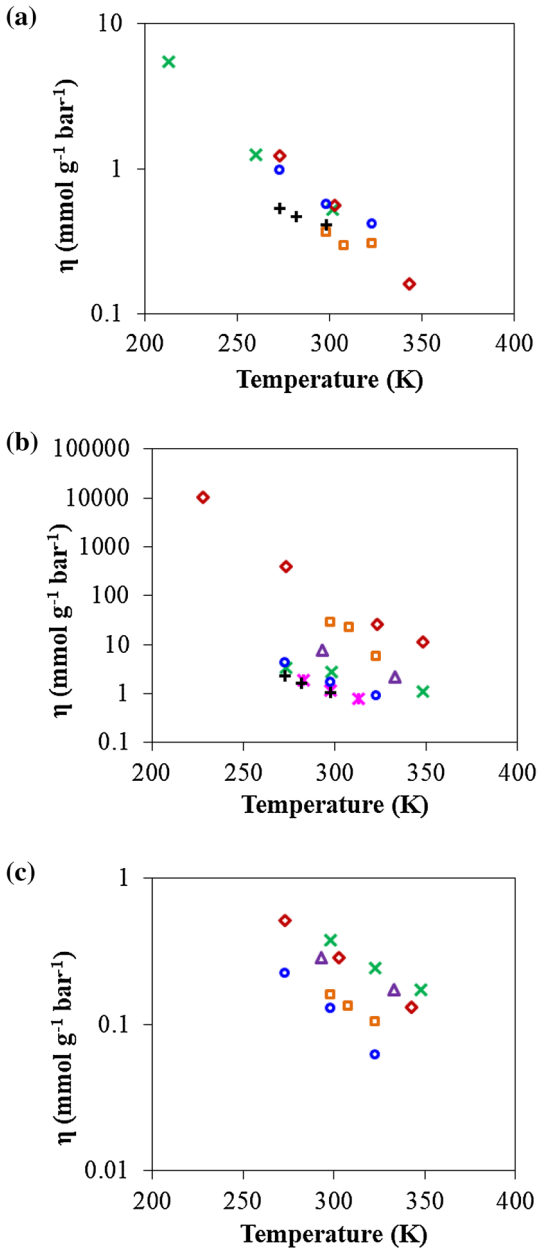

Fig. 5 Adsorption strength of **a** CH_4, **b** CO_2, and **c** N_2 in different adsorbents; silica gel (pink asterisk), activated carbon (green times), zeolite 5A (red open diamond), zeolite 13X (orange open square), Cu-BTC (purple open triangle), UiO-66 (blue open circle), and Zn-MOF (plus)

the Sips isotherm predicts well at the low adsorption region but underpredicts at the high adsorption region.

Figure 7a and b show the ratio of the observed apparent adsorption equilibrium constant to the thermodynamic adsorption equilibrium constant, ln $K/K°$, calculated from each of the isotherm data point for C_3H_8 and i-C_4H_{10} systems in Cu-BTC (Ferreira et al. 2011) respectively. For both systems, the observed ln $K/K°$ values jump in the beginning of adsorption and then quickly reach a constant value of 0 as pressure increases. One plausible explanation is that the adsorption data points at low pressure (< 0.1 bar) may be subject to higher relative uncertainty although the literature did not report the corresponding uncertainty. If the first adsorption data point at very low pressure is removed, the thermodynamic Langmuir clearly captures the isotherm data of Cu-BTC systems very well.

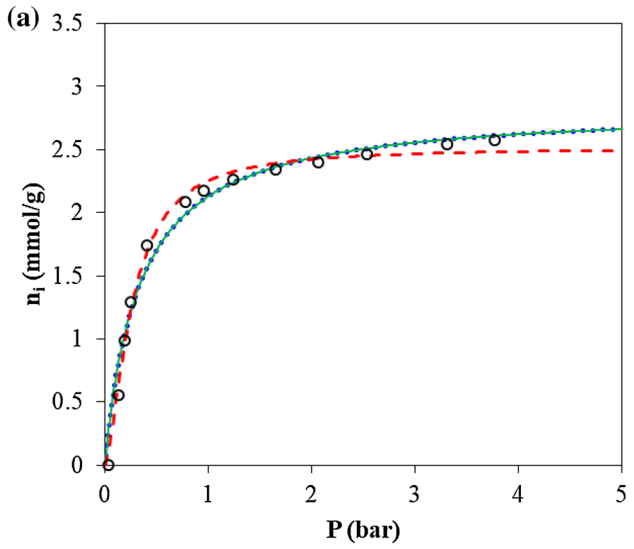

Fig. 6 Adsorption isotherm of **a** C_3H_8, **b** i-C_4H_{10} in Cu-BTC at 348 K; experimental data (open circle), Langmuir (dotted blue line), Sips (dashed red line), thermodynamic Langmuir (solid green line). Note that the Langmuir line and the thermodynamic Langmuir line overlap each other

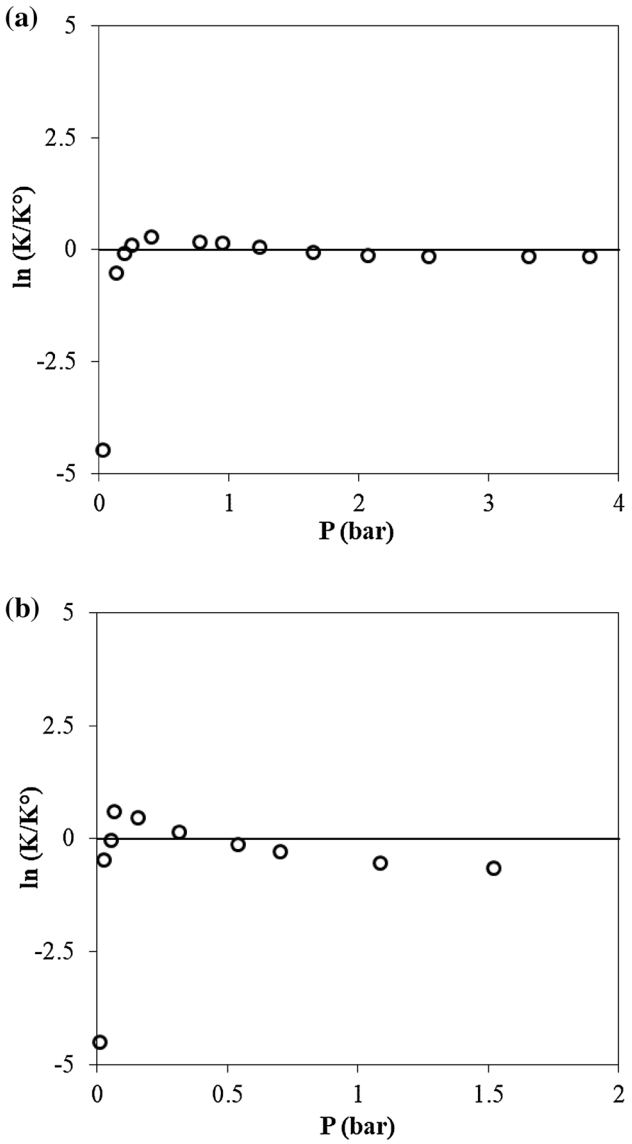

Fig. 7 Ratio of thermodynamic adsorption equilibrium constant and observed apparent adsorption equilibrium constant for **a** C_3H_8 and **b** i-C_4H_{10} adsorption with Cu-BTC at 348 K (Ferreira et al. 2011)

4 Conclusion

A thermodynamic Langmuir isotherm model is proposed by introducing the concept of activity and activity coefficient to the classical Langmuir isotherm. With three physically meaningful parameters, i.e., adsorption maximum amount n_i^0, thermodynamic adsorption equilibrium constant $K°$, and binary interaction parameter $\tau_{1\phi}$, the model accurately describes the 98 isotherms of 33 tested adsorption systems. Based on these three parameters, we further propose an adsorption strength, the product of n_i^0 and $K°$, as an intrinsic measure for selecting adsorbents for a given gas adsorption task. The proposed model is superior to the classical Langmuir isotherm model and should be very useful in accurate correlation of pure component adsorption isotherms and subsequent correlation and prediction of mixed-gas adsorption isotherms. Future work will report predictions on enthalpy of adsorption and mixed-gas adsorption equilibria from pure component adsorption isotherms represented with the thermodynamic Langmuir isotherm model.

Acknowledgements This material is based upon work supported by the U.S. Department of Energy's Office of Energy Efficiency and Renewable Energy (EERE) under the Advanced Manufacturing Office Award Number DE-EE0007888. The authors further acknowledge the financial support of the Jack Maddox Distinguished Engineering Chair Professorship in Sustainable Energy, sponsored by the J.F Maddox Foundation. C.-K. Chang acknowledges the WOCE REU program at Texas Tech University for sponsoring his research at TTU. C.-K. also acknowledges H. Kaur for insightful discussions on the aNRTL model. C.-K. further thanks Md Islam and Y. Hao for technical help in the use of Aspen Plus process simulator.

References

Al-Janabi, N., Hill, P., Torrente-Murciano, L., Garforth, A., Gorgojo, P., Siperstein, F., et al.: Mapping the Cu-BTC metal–organic framework (HKUST-1) stability envelope in the presence of water vapour for CO_2 adsorption from flue gases. Chem. Eng. J. **281**, 669–677 (2015)

Bakhtyari, A., Mofarahi, M.: Pure and binary adsorption equilibria of methane and nitrogen on zeolite 5A. J. Chem. Eng. Data **59**, 626–639 (2014)

Benard, P., Chahine, R.: Modeling of high-pressure adsorption isotherms above the critical temperature on microporous adsorbents: application to methane. Langmuir **13**, 808–813 (1997)

Britt, H., Luecke, R.: The estimation of parameters in nonlinear, implicit models. Technometrics **15**, 233–247 (1973)

Campo, M.C., Ribeiro, A.M., Ferreira, A., Santos, J.C., Lutz, C., Loureiro, J.M., et al.: New 13X zeolite for propylene/propane separation by vacuum swing adsorption. Sep. Purif. Technol. **103**, 60–70 (2013)

Cavenati, S., Grande, C.A., Rodrigues, A.E.: Adsorption equilibrium of methane, carbon dioxide, and nitrogen on zeolite 13X at high pressures. J. Chem. Eng. Data **49**, 1095–1101 (2004)

Do, D., Do, H.: Characterization of micro-mesoporous carbonaceous materials. Calculations of adsorption isotherm of hydrocarbons. Langmuir **18**, 93–99 (2002)

Ferreira, A.F., Santos, J.C., Plaza, M.G., Lamia, N., Loureiro, J.M., Rodrigues, A.E.: Suitability of Cu-BTC extrudates for propane–propylene separation by adsorption processes. Chem. Eng. J. **167**, 1–12 (2011)

Foo, K., Hameed, B.H.: Insights into the modeling of adsorption isotherm systems. Chem. Eng. J. **156**, 2–10 (2010)

Freundlich, H.: Über die adsorption in lösungen. Z. Phys. Chem. **57**, 385–470 (1907)

Hyun, S.H., Danner, R.P.: Equilibrium adsorption of ethane, ethylene, isobutane, carbon dioxide, and their binary mixtures on 13X molecular sieves. J. Chem. Eng. Data **27**, 196–200 (1982)

Kaur, H., Tun, H., Sees, M., Chen, C.-C.: Local composition activity coefficient model for mixed-gas adsorption equilibria. Adsorption **25**, 951–964 (2019)

Langmuir, I.: The adsorption of gases on plane surfaces of glass, mica and platinum. J. Am. Chem. Soc. **40**, 1361–1403 (1918)

Laukhuf, W.L., Plank, C.A.: Adsorption of carbon dioxide, acetylene, ethane, and propylene on charcoal at near room temperatures. J. Chem. Eng. Data **14**, 48–51 (1969)

Lewis, W., Gilliland, E., Chertow, B., Bareis, D.: Vapor—adsorbate equilibrium. III. The effect of temperature on the binary systems ethylene—propane, ethylene—propylene over silica gel. J. Am. Chem. Soc. **72**, 1160–1163 (1950)

Li, J.-R., Kuppler, R.J., Zhou, H.-C.: Selective gas adsorption and separation in metal–organic frameworks. Chem. Soc. Rev. **38**, 1477–1504 (2009)

Maring, B.J., Webley, P.A.: A new simplified pressure/vacuum swing adsorption model for rapid adsorbent screening for CO_2 capture applications. Int. J. Greenhouse Gas Control **15**, 16–31 (2013)

Mathias, P.M., Kumar, R., Moyer, J.D., Schork, J.M., Srinivasan, S.R., Auvil, S.R., et al.: Correlation of multicomponent gas adsorption by the dual-site Langmuir model. Application to nitrogen/oxygen adsorption on 5A-zeolite. Ind. Eng. Chem. Res. **35**, 2477–2483 (1996)

Mofarahi, M., Salehi, S.M.: Pure and binary adsorption isotherms of ethylene and ethane on zeolite 5A. Adsorpt. J. Int. Adsorpt. Soc. **19**, 101–110 (2013)

Mu, B., Walton, K.S.: Adsorption equilibrium of methane and carbon dioxide on porous metal-organic framework Zn-BTB. Adsorption **17**, 777–782 (2011)

Myers, A.L.: Prediction of adsorption of nonideal mixtures in nanoporous materials. Adsorption **11**, 37–42 (2005)

Myers, A., Prausnitz, J.M.: Thermodynamics of mixed-gas adsorption. AIChE J. **11**, 121–127 (1965)

Olivier, M.G., Jadot, R.: Adsorption of light hydrocarbons and carbon dioxide on silica gel. J. Chem. Eng. Data **42**, 230–233 (1997)

Pakseresht, S., Kazemeini, M., Akbarnejad, M.M.: Equilibrium isotherms for CO, CO_2, CH_4 and C_2H_4 on the 5A molecular sieve by a simple volumetric apparatus. Sep. Purif. Technol. **28**, 53–60 (2002)

Payne, H., Sturdevant, G., Leland, T.: Improved two-dimensional equation of state to predict adsorption of pure and mixed hydrocarbons. Ind. Eng. Chem. Fundam. **7**, 363–374 (1968)

Ravichandran, A., Khare, R., Chen, C.C.: Predicting NRTL binary interaction parameters from molecular simulations. AIChE J. **64**, 2758–2769 (2018)

Reich, R., Ziegler, W.T., Rogers, K.A.: Adsorption of methane, ethane, and ethylene gases and their binary and ternary mixtures and carbon dioxide on activated carbon at 212-301 K and pressures to 35 atmospheres. Ind. Eng. Chem. Process Des. Dev. **19**, 336–344 (1980)

Renon, H., Prausnitz, J.M.: Local compositions in thermodynamic excess functions for liquid mixtures. AIChE J. **14**, 135–144 (1968)

Silva, J.A., Rodrigues, A.E.: Sorption and diffusion of n-pentane in pellets of 5A zeolite. Ind. Eng. Chem. Res. **36**, 493–500 (1997)

Sips, R.: On the structure of a catalyst surface. J. Chem. Phys. **16**, 490–495 (1948)

Sips, R.: On the structure of a catalyst surface. II. J. Chem. Phys. **18**, 1024–1026 (1950)

Sircar, S.: Role of adsorbent heterogeneity on mixed gas adsorption. Ind. Eng. Chem. Res. **30**, 1032–1039 (1991)

Sohn, S., Kim, D.: Modification of Langmuir isotherm in solution systems—definition and utilization of concentration dependent factor. Chemosphere **58**, 115–123 (2005)

Sreńscek-Nazzal, J., Narkiewicz, U., Morawski, A.W., Wróbel, R.J., Michalkiewicz, B.: Comparison of optimized isotherm models and error functions for carbon dioxide adsorption on activated carbon. J. Chem. Eng. Data **60**, 3148–3158 (2015)

Talu, O., Zwiebel, I.: Multicomponent adsorption equilibria of nonideal mixtures. AIChE J. **32**, 1263–1276 (1986)

Toth, J.: State equation of the solid-gas interface layers. Acta Chim. Hung. **69**, 311–328 (1971)

Walton, K.S., Sholl, D.S.: Predicting multicomponent adsorption: 50 years of the ideal adsorbed solution theory. AIChE J. **61**, 2757–2762 (2015)

Wang, Y., LeVan, M.D.: Adsorption equilibrium of carbon dioxide and water vapor on zeolites 5A and 13X and silica gel: pure components. J. Chem. Eng. Data **54**, 2839–2844 (2009)

Zhang, W., Huang, H., Zhong, C., Liu, D.: Cooperative effect of temperature and linker functionality on CO_2 capture from industrial gas mixtures in metal–organic frameworks: a combined experimental and molecular simulation study. Phys. Chem. Chem. Phys. **14**, 2317–2325 (2012)

Zhang, Z., Zhou, J., Xing, W., Xue, Q., Yan, Z., Zhuo, S., et al.: Critical role of small micropores in high CO_2 uptake. Phys. Chem. Chem. Phys. **15**, 2523–2529 (2013)